

Energetics of the Thermal Dimerization of Acenaphthylene to Heptacyclene

Rui C. Santos,[†] Carlos E. S. Bernardes,[‡] Hermínio P. Diogo,[†] M. Fátima M. Piedade,^{†,‡} José. N. Canongia Lopes,[†] and Manuel E. Minas da Piedade^{*,‡}

Centro de Química Estrutural, Complexo Interdisciplinar, Instituto Superior Técnico, 1049-001 Lisboa, Portugal, and Departamento de Química e Bioquímica, Faculdade de Ciências, Universidade de Lisboa, 1649-016 Lisboa, Portugal

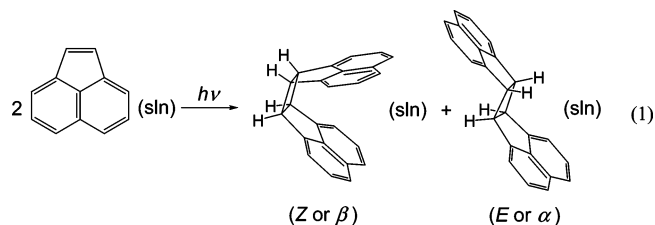
Received: October 31, 2005; In Final Form: December 14, 2005

The energetics of the thermal dimerization of acenaphthylene to give *Z*- or *E*-heptacyclene was investigated. The standard molar enthalpy of the formation of monoclinic *Z*- and *E*-heptacyclene isomers at 298.15 K was determined as $\Delta_f H_m^{\circ}(E-C_{24}H_{16}, cr) = 269.3 \pm 5.6 \text{ kJ}\cdot\text{mol}^{-1}$ and $\Delta_f H_m^{\circ}(Z-C_{24}H_{16}, cr) = 317.7 \pm 5.6 \text{ kJ}\cdot\text{mol}^{-1}$, respectively, by microcombustion calorimetry. The corresponding enthalpies of sublimation, $\Delta_{sub} H_m^{\circ}(E-C_{24}H_{16}) = (149.0 \pm 3.1) \text{ kJ}\cdot\text{mol}^{-1}$ and $\Delta_{sub} H_m^{\circ}(Z-C_{24}H_{16}) = (128.5 \pm 2.3) \text{ kJ}\cdot\text{mol}^{-1}$ were also obtained by Knudsen effusion and Calvet-drop microcalorimetry methods, leading to $\Delta_f H_m^{\circ}(E-C_{24}H_{16}, g) = (418.3 \pm 6.4) \text{ kJ}\cdot\text{mol}^{-1}$ and $\Delta_f H_m^{\circ}(Z-C_{24}H_{16}, g) = (446.2 \pm 6.1) \text{ kJ}\cdot\text{mol}^{-1}$, respectively. These results, in conjunction with the reported enthalpies of formation of solid and gaseous acenaphthylene, and the entropies of acenaphthylene and both heptacyclene isomers obtained by the B3LYP/6-31G(d,p) method led to the conclusion that at 298.15 K the thermal dimerization of acenaphthylene is considerably exothermic and exergonic in the solid and gaseous states (although more favorable when the *E* isomer is the product), suggesting that the nonobservation of the reaction under these conditions is of kinetic nature. A full determination of the molecular and crystal structure of the *E* dimer by X-ray diffraction is reported for the first time. Finally, molecular dynamics computer simulations on acenaphthylene and the heptacyclene solids were carried out and the results discussed in light of the corresponding structural and $\Delta_{sub} H_m^{\circ}$ data experimentally obtained.

Introduction

The dimerization of acenaphthylene in solution upon exposure to sunlight (eq 1) was observed and reported for the first time over 90 years ago by Dziejowski and co-workers.^{1,2} These authors were able to show that the reaction leads to two isomeric cyclobutane dimers and that the relative yields of the products strongly depend on the solvent and on the acenaphthylene concentration.² Due to the presence of the seven rings, the compounds were dubbed heptacyclenes. The dimer with the higher fusion temperature ($T_f = 579\text{--}580 \text{ K}$) was named α -heptacyclene² and was later shown to correspond to the *E* form in eq 1 (cyclobuta[1,2-a:3,4-a']diacenaphthylene, 6b,6c-12b,12c-tetrahydro-(6b α ,6c β ,12b β ,12c α), CAS Registry Number, 14620-98-5) from a partial determination of the molecular structure by X-ray diffraction.³ The compound with the lower fusion temperature ($T_f = 505\text{--}507 \text{ K}$) was designated by β -heptacyclene (cyclobuta[1,2-a:3,4-a']diacenaphthylene, 6b,6c,12b,12c-tetrahydro-(6b α ,6c α ,12b α ,12c α), CAS Registry Number, 15065-28-8). The assignment of the *Z* structure to β -heptacyclene was first based on the results of ozonolysis studies⁴ and was subsequently supported by an X-ray diffraction determination of the molecular structure.⁵

A variety of studies have been undertaken to elucidate the mechanism of the photodimerization of acenaphthylene and of the reverse photodissociation of the dimers in solution.^{6–14} Practically unexplored are, however, the thermal aspects of the acenaphthylene/heptacyclene system, although Dziejowski and



Paschalski² had already noted that acenaphthylene can be regenerated by decomposition of the *E* dimer upon heating to its fusion temperature in an open vessel. If the reaction is carried out in a closed tube, then only products resulting from the subsequent polymerization of acenaphthylene are observed.²

In this work, the energetics of the interconversion between acenaphthylene and the *E* or *Z* dimers in the solid and gaseous states was investigated, by combining the results of combustion calorimetry, Calvet-drop microcalorimetry, and Knudsen effusion measurements, with data from density functional theory and molecular simulation calculations. In addition, a full determination of the molecular and crystal structure of the *E* dimer by X-ray diffraction is reported for the first time.

Methods

General. Elemental analyses were carried out on a Fisons Instruments EA1108 apparatus. The IR spectra were recorded in a Jasco 430 spectrophotometer calibrated with polystyrene film, using KBr plates. The ¹H NMR spectra were obtained at ambient temperature on a Varian 300 MHz spectrometer. X-ray powder diffractometry (XRD) was carried out over the range $5^{\circ} \leq 2\theta \leq 35^{\circ}$, on a Rigaku diffractometer employing Cu K α

* To whom correspondence should be addressed. E-mail: memp@fc.ul.pt.

[†] Instituto Superior Técnico.

[‡] Universidade de Lisboa.

radiation ($\lambda = 1.540598 \text{ \AA}$). The indexing of the powder patterns was performed using the program Checkcell.¹⁵ Differential scanning calorimetry (DSC) measurements were made with a 2920 MTDSC temperature-modulated apparatus from TA Instruments operated as a conventional DSC.

Materials. Benzene (Merck, p.a.), ethanol (Merck, p.a.), hexane (J. M. Gomes dos Santos), and dichloromethane (J. M. Gomes dos Santos, 99.8%) were used without further purification. Crude acenaphthylene (Aldrich, 75%, with 20% acenaphthene content) was reacted with picric acid (Aldrich, 99+%) in benzene to precipitate the corresponding picrate.^{8,16} The obtained solid was washed with ethanol and treated with a concentrated aqueous ammonia solution at room temperature. The precipitated acenaphthylene was recrystallized from hexane and purified by sublimation at 323 K and 0.4 Pa.

The *E* and *Z* dimers were obtained by a method adapted from the literature.^{1,9,12} A solution of 33 g of acenaphthylene in 1 dm³ of benzene (0.2 M) was placed inside a 2 dm³ three-neck round-bottom flask and exposed to sunlight for 30 days. Well-formed white needles of the *E* dimer were found at the bottom of the flask at the end of this period. These were separated from the solution by decantation, washed with ethanol, and dried in a vacuum at 333 K and 13 Pa. The mother liquor was transferred to a silica gel 60 (Merck, 230-400 mesh ASTM) column with a length of 50 cm and a diameter of 8 cm and chromatographed using hexane/dichloromethane as the eluent. The elution was started with pure hexane, and a progressive increase of the mass fraction of dichloromethane up to 100% enabled the separation of acenaphthylene and the dimers. Concentration of the hexane/dichloromethane fraction containing the *E* dimer at reduced pressure yielded white needles of the compound, which were isolated by decantation and washed twice with boiling cyclohexane. These were combined with those of the first crop (see above), recrystallized from benzene, and dried in a vacuum (at 313 K and 0.4 Pa). The fraction containing the *Z* dimer was taken to dryness, and the product was purified by repeated dissolution in boiling benzene and precipitation by the addition of cold methanol. *E*-Heptacyclene: Anal. Calcd for C₂₄H₁₆: C, 94.61; H, 5.29. Found: C, 94.74; H, 5.26. ¹H NMR (300 MHz, CDCl₃/TMS): δ /ppm 7.75 (dd, 4H), 7.62 (dd, 4H), 7.53 (dd, 4H), 4.10 (s, 4H). The powder pattern was indexed as monoclinic, space group *P*₂₁/*n*, with *a* = 7.8616 pm, *b* = 4.8716 pm, *c* = 20.3190 pm, and β = 92.68°. The good agreement between these values and *a* = 7.8270 pm, *b* = 4.8647 pm, *c* = 20.2212 pm, and β = 92.79°, obtained in this work from single-crystal X-ray diffraction experiments (see below), indicated that the sample was phase pure. The temperatures of fusion of the sample obtained by DSC at the onset (*T*_{on}) and at the peak of the measuring curve (*T*_{max}) were *T*_{on} = (587.22 ± 0.06) K and *T*_{max} = (587.56 ± 0.02) K. The uncertainties quoted for both values represent twice the standard deviation of the mean of four independent determinations. *Z*-Heptacyclene: Anal. Calcd for C₂₄H₁₆: C, 94.61; H, 5.29. Found: C, 94.90; H, 5.33. ¹H NMR (300 MHz, CDCl₃/TMS): δ /ppm 7.73 (dd, 4H), 7.60 (dd, 4H), 7.52 (dd, 4H), 4.82 (s, 4H). The powder pattern was indexed as monoclinic, space group *P*₂₁/*c*, with *a* = 11.9665 Å, *b* = 13.9305 Å, *c* = 10.0035 Å, and β = 107.7°. These values are in excellent agreement with those reported from single-crystal X-ray diffraction experiments (*a* = 11.966 Å, *b* = 13.930 Å, *c* = 10.003 Å, β = 107.7°).⁵ The DSC determination of the temperature of fusion gave *T*_{on} = (505.47 ± 0.11) K and *T*_{max} = (506.78 ± 0.02) K. The uncertainties quoted for both values represent twice the standard deviation of the mean of five independent determinations.

TABLE 1: Crystallographic Data for *E*-Heptacyclene^a

empirical formula	C ₁₂ H ₈
formula weight	152.18
temp/K	293 K
crystal size/mm	0.3 × 0.15 × 0.08
color of crystal	colorless
crystal system	monoclinic
space group	<i>P</i> ₂ ₁ / <i>n</i>
<i>a</i> /Å	7.8270(5)
<i>b</i> /Å	4.8647(5)
<i>c</i> /Å	20.2212(16)
β /deg	92.791(6)
<i>V</i> /Å ³	769.03(11)
<i>Z</i>	4
$\rho_{\text{calcd}}/\text{g}\cdot\text{cm}^{-3}$	1.314
2 θ limits/deg	4.38–67.08
μ/mm^{-1}	0.564
reflections collected/unique	2628/1315 (<i>R</i> (int) = 0.0620)
data/restraints/parameters	1315/0/142
final <i>R</i> indices [<i>I</i> > 2 σ (<i>I</i>)]	<i>R</i> ₁ = 0.0367; w <i>R</i> ₂ = 0.0858
GOF on <i>F</i> ²	1.015
extinction coefficient	0.0201(15)
largest diff. peak and hole	0.139 and −0.119 e. Å ^{−3}

^a There is half of a molecule in the asymmetric unit.

Crystal Structure Determination. A single crystal of the *E* dimer, suitable for X-ray structure determination, was selected from those obtained at the end of the irradiation phase of the synthesis mentioned above. Data were collected using an Enraf-Nonius TURBOCAD4 diffractometer with Cu K α radiation ($\lambda = 1.54180 \text{ \AA}$). The unit cell dimensions and orientation matrix were obtained by least-squares refinement of 25 centered reflections with $14.37 < \theta < 24.64^\circ$.

The crystal structure was solved by direct methods, using the SIR97 program,¹⁷ and refined by SHELXL97 (full-matrix least-squares refinements),¹⁸ both included in the package WinGX-Version 1.64.03b.¹⁹ All non-hydrogen atoms were refined anisotropically and the hydrogen atoms were located in the Fourier maps and refined isotropically. Further details of the crystal structure determination are given in Table 1. Graphical representations were prepared using ORTEPIII²⁰ and Mercury 1.1.2.²¹

Enthalpy of Sublimation Measurements. The enthalpies of sublimation of *E*- and *Z*-heptacyclene were determined by using the Knudsen effusion apparatus and operating procedure previously described.²² The temperature of the tubular furnace surrounding the brass block containing the effusion cells (up to three cells with effusion holes of different dimensions can be inserted in the block) was controlled to better than ±0.1 K by a Eurotherm 902P thermostatic unit and a K-type thermocouple placed in contact with the inner wall of the furnace. The equilibrium temperature inside the cell was assumed to be identical to the temperature of the brass block. This temperature was measured with a precision of ±0.1 K by a Tecnis 100 Ω platinum resistance thermometer embedded in the block and connected in a four wire configuration to a Keithley 2000 multimeter. The cell was initially charged with ca. 0.2 g of sample, and the mass loss in each run was determined to ±10^{−5} g with a Mettler AT201 balance.

The enthalpy of sublimation of *Z*-heptacyclene was also determined using the Calvet-drop method.²³ In this case, each run involved the recording of three measuring curves corresponding to the pumping background, the electrical calibration, and the sublimation of the sample, respectively.²³ These measuring curves were plots of the differential output of the thermopile detectors surrounding the reference and sample cells as a function of time. In the main experiment, a thin capillary

containing 1.2–4.3 mg of *Z*-heptacyclene was weighed to $\pm 10^{-6}$ g with a Mettler M5 balance and dropped into the sample cell under nitrogen atmosphere at 405.8 K. An endothermic peak due to the heating of the sample from room temperature to 405.8 K was first observed. After the signal returned to the baseline, the cells were evacuated and the measuring curve corresponding to the sublimation of *Z*-heptacyclene was acquired. No unsublimed or decomposed sample was found inside the cell at the end of the experiments.

Combustion Calorimetry. The standard energies of combustion of *E*- and *Z*-heptacyclene were measured by microcombustion calorimetry. Details of the apparatus and the general experimental procedure have been reported.²⁴ In a typical experiment, a pellet of the compound under study (*E*-heptacyclene, 17.5–41.7 mg; *Z*-heptacyclene, 14.3–27.2 mg) and, except in two of the experiments with *Z*-heptacyclene, a drop of *n*-hexadecane (B.D.H., ca. 3.1–4.9 mg in the case of *E*-heptacyclene and 0.0–7.2 mg in the case of *Z*-heptacyclene) were placed in a Pt crucible and weighed to 0.1 μ g in a Sartorius 4504 Mp8-1 ultra-micro balance. The crucible with the sample was transferred to the sample holder in the bomb head. A volume of 50 μ L of distilled and deionized water from a Millipore system (conductivity 0.1 μ S) was introduced into the bomb body. The stainless steel bomb of 17.95 cm³ internal volume was closed and purged twice by successively charging it with oxygen at a pressure of 1.01 MPa and venting the overpressure. After purging, the bomb was charged with oxygen at a pressure of 3.04 MPa and introduced into the calorimeter. The ignition of the sample was initiated by a discharge of a 2200 μ F capacitor through a platinum wire. The duration of the initial, main, and final periods of the experiment was 30 min each. The HNO₃ formed from traces of atmospheric N₂ remaining inside the bomb after purging with O₂ was determined as NO₃⁻, using a Dionex 4000i ion chromatography apparatus.

Density Functional Theory (DFT) Calculations. DFT calculations were performed using the Gaussian-98 package, revision A.8.²⁵ The geometry optimizations and the calculations of the total energies were made using the Becke's three-parameter hybrid method²⁶ with the Perdew and Wang PW91²⁷ correlation functional (B3PW91) and the Lee, Yang, and Parr LYP²⁸ correlation functional (B3LYP). Total energies (*E*) were obtained from eq 2²⁹

$$E = V_{\text{NN}} + H^{\text{CORE}} + V_{\text{ee}} + E_{\text{X}}[\rho] + E_{\text{C}}[\rho] \quad (2)$$

where V_{NN} is the nuclear–nuclear interaction, H^{CORE} is a mono-electronic contribution to the total energy, including electron kinetic and electron–nuclear interaction energies, and V_{ee} is the Coulombic interaction between the electrons. The terms $E_{\text{X}}[\rho]$ and $E_{\text{C}}[\rho]$ represent the exchange and correlation energies, respectively, functionals of the electronic density ρ . Full geometry optimizations have been carried out with the 6-31G(d,p)³⁰ and cc-pVDZ³¹ basis sets. The corresponding total energies were corrected with zero-point vibrational energies (ZPEs) and thermal energy corrections (without frequency scaling) calculated at the same theoretical level. Single-point energy calculations with the cc-pVTZ³¹ basis set using geometries, zero-point energy, and thermal energy corrections obtained using the cc-pVDZ basis set were also made.

Molecular Dynamics (MD) Simulation Methods. Molecular dynamics simulations were carried out using the DL_POLY package.³² Several MD runs were performed to estimate the sublimation enthalpy of *Z*-heptacyclene, *E*-heptacyclene, and acenaphthylene crystals at 298.15 K. The initial configuration

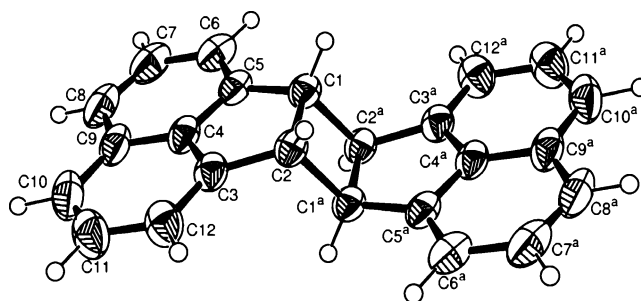


Figure 1. ORTEP²⁰ of *E*-heptacyclene with labeling scheme.

of all runs corresponded to that of the crystal geometries obtained by X-ray diffraction in this work for *E*-heptacyclene, or reported in the literature for *Z*-heptacyclene⁵ and acenaphthylene.³³

In the case of the *Z* dimer, the simulation box was composed of 8 unit cells ($2 \times 2 \times 2$ cells in the *a*, *b*, and *c* directions, respectively) with a total of 32 molecules (1280 atoms). The simulations with the *E* dimer used boxes containing 15 unit cells ($3 \times 5 \times 1$) with 30 molecules (1200 atoms). For acenaphthylene, the simulation box consisted of 9 unit cells ($3 \times 3 \times 1$ cells in the *a*, *b*, and *c* directions, respectively), with a total of 72 molecules (1440 atoms). The cutoff distance in all cases was set to 900 pm. Beyond this distance, standard long-range force evaluation techniques were employed (including Ewald summation in the cases where Coulombic interactions were incorporated in the model). The time step used in all simulation runs was 2 fs, with an equilibration time of 100 ps, followed by production cycles of another 100 ps.

The molecules were set as rigid units, and the intermolecular interactions were modeled by three different force fields: a Buckingham (exp-6) potential parametrized for carbon and hydrogen atoms by Williams and Cox (W&C),³⁴ a Lennard-Jones potential with an additional electrostatic term, parametrized by Jorgensen, Maxwell, and Tirado-Rives, and known as the OPLS all-atom (OPLS-AA) force-field,³⁵ and finally the same OPLS-AA force field without the electrostatic contribution (i.e., atomic point charges set to zero) and hitherto referred as OPLS-AA-q (minus "q"). The W&C force field is a well-tested potential for the study of intermolecular forces in organic molecular crystals. On the other hand, the OPLS-AA force field is normally used to model liquids or dense gases (in general the repulsive part of the Lennard-Jones potential is not steep enough to deal with the dense packing found in crystals). It was employed in this work to test if a cruder, but also more general and widely used, potential was able to predict the geometry and energetics of simple molecular crystals with acceptable accuracy.

Results and Discussion

Structure. The results of the X-ray diffraction study of *E*-heptacyclene show that the asymmetric unit consists of half of the molecule, with the all molecule being generated by an inversion center located at the center of the four-membered ring. This ring lies almost in the (010) plane (the angle between the two planes is 20.84 °), and the planar system formed by the five- and six-membered rings is inclined at 44.5 °, relative to the (010) plane, as was suggested in a preliminary X-ray analysis.³ The ORTEP²⁰ drawing and labeling scheme of the molecule are represented in Figure 1. The aliphatic single bond distances in the four-membered ring of 1.5712(16) Å (C1–C2) and 1.5652(17) Å (C1–C2^a) are similar to those reported for the corresponding bonds in *Z*-heptacyclene (C1–C2, 1.561 Å;

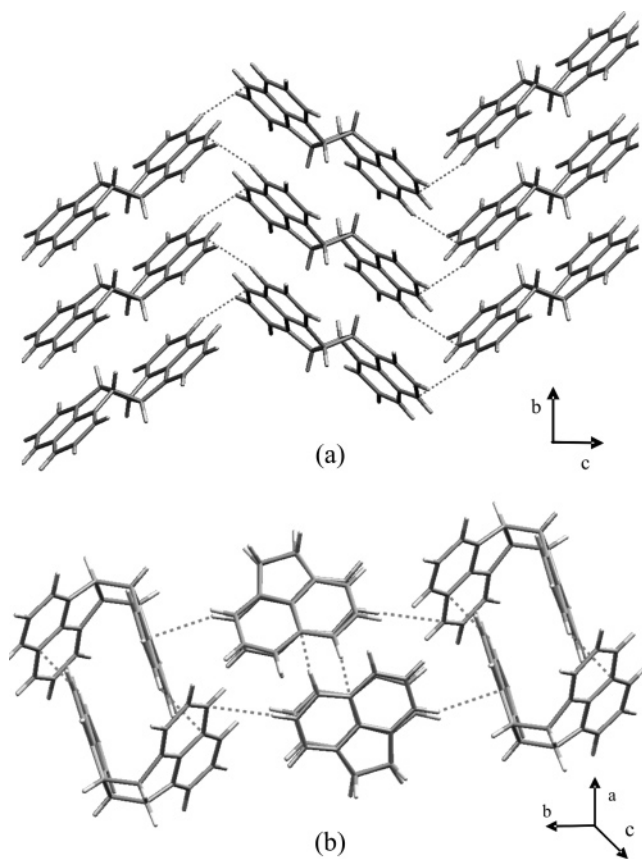


Figure 2. Molecular packing obtained from the experimental data with Mercury 1.1.2²¹ of (a) *E*-heptacyclene and (b) *Z*-heptacyclene.

C1–C2^a, 1.551 Å)⁵ and in acenaphthene (C1–C2, 1.540 Å, from X-ray diffraction; C1–C2, 1.576 and 1.552 Å, from neutron diffraction studies).^{36,37} The four-membered ring structure in *E*-heptacyclene exhibits internal angles of 90° as it is also found in *Z*-heptacyclene.⁵ The angles C3–C2–C1^a (115.86(10)°), C5–C1–C2^a (115.56(10)°), C3^a–C2^a–C1 (115.86(10)°), and C5^a–C1^a–C2 (115.56(10)°) in *E*-heptacyclene are smaller than the corresponding angles in *Z*-heptacyclene (118.13°, 118.35°, 117.71°, and 118.85, respectively) probably due to steric hindrance in the latter molecule. The acenaphthenic unit of *E*-heptacyclene is essentially planar (the greatest deviation from the plane is 0.0216 Å and corresponds to atom C5) and forms an angle of 64.4° with the plane of the four-membered ring.

The B3LYP/6-31G(d,p), B3PW91/6-31G(d,p), and B3LYP/cc-pVDZ methods reproduce the bond distances and angles of the C–C skeleton of *E*- and *Z*-heptacyclene with average deviations smaller than 0.02 Å and 1°, respectively. The molecules computed symmetry is C_{2h} in the case of the *E* isomer and C_{2v} for the *Z* isomer. A full comparison of all bond distances and angles in *E*-heptacyclene with those obtained for *Z*-heptacyclene or acenaphthene by X-ray diffraction, neutron diffraction, or computational chemistry methods is included in the Supporting Information. The molecular packing in *E*-heptacyclene (Figure 2a) shows that the molecule forms zigzag chains along the (101) plane, through an intermolecular contact C10–H10...C8 (2.525 Å); the same type of interaction also connects the zigzag chains between them. There is a weak C–H... π interaction of 3.622 Å between the C10–H10 bond and the centroid of the five-membered ring of the molecule, which acts as the hydrogen bond acceptor. In the case of *Z*-heptacyclene, the molecules are packed in rows along the (101) plane in a line of centers of symmetry. There are also some intermolecular contacts of the type C–H...C that range from 2.817 to 2.893

Å. Although the interactions that can be found in both the packings of the *E* and *Z* isomers are very weak, there are more intermolecular contacts in the crystalline structure of the *E* isomer than in that of the *Z* isomer. The crystalline structure of *E*-heptacyclene is also much more ordered than that of *Z*-heptacyclene. These conclusions are in line with the fact that the enthalpy of sublimation of *E*-heptacyclene is 20.5 kJ·mol^{−1} larger than that of *Z*-heptacyclene (see below).

Energetics. The 2001 IUPAC recommended standard atomic masses were used in the calculation of all molar quantities.³⁸ The standard molar enthalpies of combustion of *Z*- and *E*-heptacyclene at 298.15 K, obtained in this work, are shown in Table 2 (see Supporting Information for details). The uncertainties quoted represent twice the overall standard deviation of the mean of seven and five results, respectively, and include the contributions from the energy of combustion of benzoic acid and from the calibration experiments.³⁹ These values refer to reaction 3



and lead to the corresponding enthalpies of formation in the crystalline state (Table 2) by using $\Delta_f H_m^\circ(\text{CO}_2, \text{g}) = -(393.51 \pm 0.13)$ kJ·mol^{−1}⁴⁰ and $\Delta_f H_m^\circ(\text{H}_2\text{O}, \text{l}) = -(285.830 \pm 0.040)$ kJ·mol^{−1}.⁴⁰

The vapor pressures, p , of the *Z*- and *E*-heptacyclene isomers obtained in the Knudsen effusion experiments (see Supporting Information) were calculated from⁴¹

$$p = \frac{m}{At} \left(\frac{2\pi RT}{M} \right)^{1/2} \left(\frac{8r + 3l}{8r} \right) \left(\frac{2\lambda}{2\lambda + 0.48r} \right) \quad (4)$$

where m is the mass loss during time t , A , l , and r are the area, the thickness, and the radius of the effusion hole, respectively, M is the molar mass of the compound under study, R is the gas constant, T is the absolute temperature, and λ is the mean free path given by⁴²

$$\lambda = \frac{kT}{\sqrt{2} \pi \sigma^2 p} \quad (5)$$

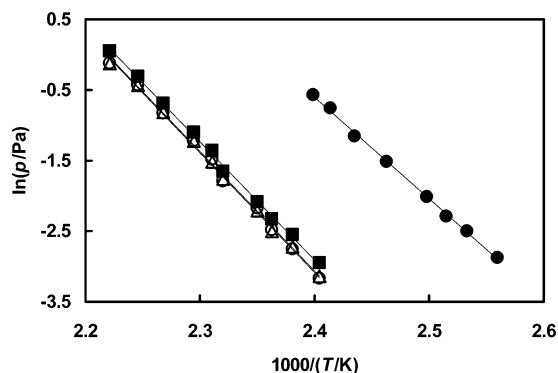
Here, k represents the Boltzmann constant and σ the collision diameter. The collision diameter of *Z*- and *E*-heptacyclene were estimated as 770 and 769 pm, respectively, from the van der Waals volume of the molecules calculated with the GEPOL93 program.⁴³ In the experiments with *E*-heptacyclene, three cells with different effusion holes were simultaneously used. The dimensions of the holes were as follows: hole 1, $A = 6.94 \times 10^{-7}$ m², $l = 2.09 \times 10^{-5}$ m, and $r = 4.70 \times 10^{-6}$ m; hole 2, $A = 4.39 \times 10^{-7}$ m², $l = 2.09 \times 10^{-5}$ m, and $r = 3.74 \times 10^{-6}$ m; and hole 3, $A = 7.39 \times 10^{-7}$ m², $l = 2.09 \times 10^{-5}$ m, and $r = 4.85 \times 10^{-6}$ m. Only hole 3 was used in the case of *Z*-heptacyclene. The vapor pressure against temperature data obtained for both isomers data were fitted to eq 6⁴⁴

$$\ln p = a + \frac{b}{T} \quad (6)$$

leading to the results in Figure 3 and Table 3. The enthalpies of sublimation of *Z*- and *E*-heptacyclene at T_m (the average of the highest and lowest temperatures of the range covered in each series of experiments) are given by $\Delta_{\text{sub}} H_m^\circ(T_m) = bR$ and the uncertainties quoted for a , b , and the enthalpy of sublimation include Student's factor for 95% confidence level.⁴⁵ The corresponding $\Delta_{\text{sub}} H_m^\circ$ values at 298.15 K were derived from

TABLE 2: Standard Molar Enthalpies of Combustion, Formation, and Sublimation of *Z*- and *E*-Heptacyclene and Acenaphthylene at 298.15 K (data in kJ·mol⁻¹)

compound	$-\Delta_c H_m^o$	$\Delta_f H_m^o(\text{cr})$	$\Delta_{\text{sub}} H_m^o$	$\Delta_f H_m^o(\text{g})$
<i>Z</i> -heptacyclene	12048.59 ± 4.63	317.7 ± 5.6	128.5 ± 2.3	446.2 ± 6.1
<i>E</i> -heptacyclene	12000.22 ± 4.70	269.3 ± 5.6	149.0 ± 3.1	418.3 ± 6.4
acenaphthylene		190.8 ± 3.4 ^a	72.97 ± 0.33 ^{a,b}	263.8 ± 3.4 ^a

^a Reference 48. ^b Reference 49.**Figure 3.** Vapor pressures of *Z*-heptacyclene (●, hole 3) and *E*-heptacyclene (○, hole 1; ■, hole 2; △, hole 3) as a function of temperature.**TABLE 3: Values of the Constants in Eq 6 and Enthalpies of Sublimation of *Z*- and *E*-Heptacyclene Obtained by the Knudsen Effusion Method**

isomer	T_m/K	a	$-b$	$\Delta_{\text{sub}} H_m^o(T_m)/\text{kJ}\cdot\text{mol}^{-1}$
<i>E</i> -heptacyclene (hole 1)	433.1	37.54 ± 1.66	16921.0 ± 717.8	140.7 ± 6.0
<i>E</i> -heptacyclene (hole 2)	433.1	37.31 ± 1.37	16757.9 ± 593.8	139.3 ± 4.9
<i>E</i> -heptacyclene (hole 3)	433.1	37.43 ± 1.45	16871.1 ± 625.9	140.3 ± 5.2, 140.0 ± 3.1 ^a
<i>Z</i> -heptacyclene (hole 3)	403.8	34.09 ± 1.25	14454.9 ± 506.0	120.2 ± 4.2

^a Weighed mean of the three results obtained for *E*-heptacyclene.

$$\Delta_{\text{sub}} H_m^o(298.15 \text{ K}) = \Delta_{\text{sub}} H_m^o(T) + \int_T^{298.15 \text{ K}} [C_{p,m}^o(\text{g}) - C_{p,m}^o(\text{cr})] dT \quad (7)$$

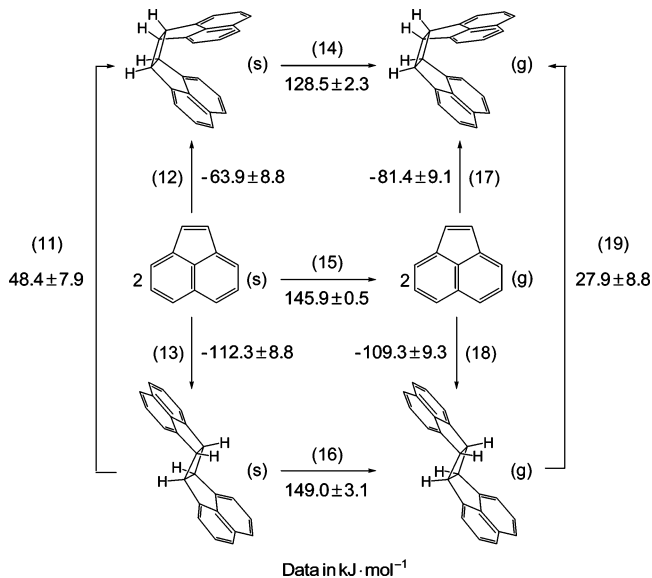
where $C_{p,m}^o(\text{cr})$ and $C_{p,m}^o(\text{g})$ are the molar heat capacities of the compounds in the crystalline and gaseous states, respectively. The temperature dependences of the heat capacities in eq 7 were estimated as ($C_{p,m}^o$ in J·mol⁻¹·K⁻¹)

$$C_{p,m}^o(\text{Z- and E-heptacyclene, cr}) = -7.6745 \times 10^{-4} T^2 + 1.7551 T - 87.840 \quad (8)$$

$$C_{p,m}^o(\text{Z-heptacyclene, g}) = -7.8911 \times 10^{-4} T^2 + 1.6338 T - 107.12 \quad (9)$$

$$C_{p,m}^o(\text{E-heptacyclene, g}) = -7.8509 \times 10^{-4} T^2 + 1.6286 T - 105.61 \quad (10)$$

Equation 8 was obtained by assuming that the heat capacities of crystalline *Z*- and *E*-heptacyclene at a given temperature were twice the corresponding value for acenaphthylene in the range 273–330 K.⁴⁶ Equations 9 and 10 were based on the $C_{p,m}^o$ data obtained in the range 200–900 K, using vibrational frequencies of *Z*- and *E*-heptacyclene obtained by the B3LYP/6-31G(d,p) method and scaled by 0.9620.⁴⁷ Hence, $\Delta_{\text{sub}} H_m^o(\text{Z-heptacyclene}, T_m) = 120.2 \pm 4.2 \text{ kJ}\cdot\text{mol}^{-1}$ and $\Delta_{\text{sub}} H_m^o(\text{E-heptacyclene},$

SCHEME 1

$T_m) = 140.0 \pm 3.1 \text{ kJ}\cdot\text{mol}^{-1}$ lead to $\Delta_{\text{sub}} H_m^o(\text{Z-heptacyclene}) = 126.5 \pm 4.2 \text{ kJ}\cdot\text{mol}^{-1}$ and $\Delta_{\text{sub}} H_m^o(\text{E-heptacyclene}) = 149.0 \pm 3.1 \text{ kJ}\cdot\text{mol}^{-1}$ at 298.15 K.

The enthalpy of sublimation of *Z*-heptacyclene was also measured by Calvet drop-sublimation microcalorimetry, at 405.8 K, leading to $\Delta_{\text{sub}} H_m^o(\text{Z-heptacyclene}, 405.8 \text{ K}) = 122.9 \pm 2.7 \text{ kJ}\cdot\text{mol}^{-1}$ (the study of the *E* isomer was found to be outside the operating temperature range of the apparatus). The uncertainties quoted represent twice the standard deviation of the mean of eight independent results. Correction of this value to 298.15 K using the heat capacity data indicated above leads to $\Delta_{\text{sub}} H_m^o(\text{Z-heptacyclene}) = 129.3 \pm 2.7 \text{ kJ}\cdot\text{mol}^{-1}$, in good agreement with the corresponding value obtained by the Knudsen effusion method. The weighted mean of the results from both techniques $\Delta_{\text{sub}} H_m^o(\text{Z-heptacyclene}) = 128.5 \pm 2.3 \text{ kJ}\cdot\text{mol}^{-1}$ was selected in this work (Table 2).

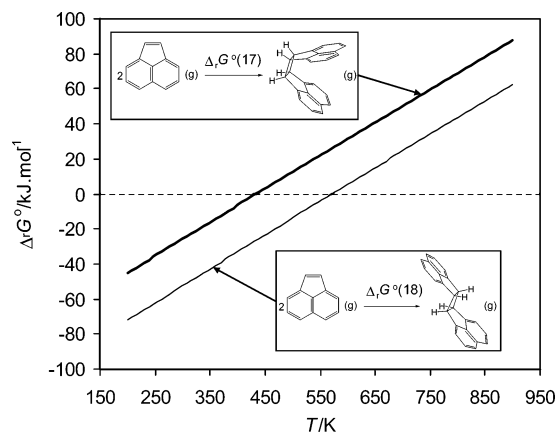
Also indicated in Table 2 are the enthalpies of formation of *Z*- and *E*-heptacyclene in the gaseous state at 298.15 K that were derived from the corresponding $\Delta_f H_m^o(\text{cr})$ and $\Delta_{\text{sub}} H_m^o$ and the reported enthalpies of formation and sublimation of acenaphthylene.^{48,49} The data in Table 2 allow us to analyze the energetics of the processes corresponding to eqs 11–19 in Scheme 1 and indicate that on enthalpic grounds the *E*-heptacyclene isomer is $27.9 \pm 8.8 \text{ kJ}\cdot\text{mol}^{-1}$ more stable than its *Z* counterpart. A similar conclusion is reached by considering the results of several theoretical models, which give enthalpies of isomerization 13.0 – $14.4 \text{ kJ}\cdot\text{mol}^{-1}$ lower than the corresponding experimental value, although considerably smaller discrepancies are found (4.2 – $5.6 \text{ kJ}\cdot\text{mol}^{-1}$) if the uncertainty interval is considered (Table 4).

The results in Table 2 also allow the analysis of the energetics of interconversion between acenaphthylene and the *E* or *Z* dimers, in the standard state, at 298.15 K, as summarized in Scheme 1. As shown in this scheme, the dimerization of

TABLE 4: Theoretical and Experimental Enthalpies of the *E*-Heptacyclene → *Z*-Heptacyclene Conversion in the Gaseous State at 298.15 K (see also Scheme 1)^a

method	$\Delta_r H_m^\circ(19)$
experimental	27.9 ± 8.8
B3LYP/6-31G(d,p)	12.9
B3PW91/6-31G(d,p)	13.8
B3LYP/cc-pVDZ	13.4
B3LYP/cc-pVTZ//B3LYP/cc-pVDZ	14.3^b

^a Data in $\text{kJ}\cdot\text{mol}^{-1}$. ^b Zero-point energy and thermal energy corrections obtained using the cc-pVDZ basis (see Supporting Information).

**Figure 4.** Standard molar Gibbs energy changes for reactions 17 and 18 as a function of temperature.

acenaphthylene to give *E*- or *Z*-heptacyclene is exothermic in the solid and gaseous states. By the use of the gas-phase entropy data $S_m^\circ(E\text{-heptacyclene, g}) = 529.3 \text{ J}\cdot\text{K}^{-1}\cdot\text{mol}^{-1}$, $S_m^\circ(Z\text{-heptacyclene, g}) = 532.7 \text{ J}\cdot\text{K}^{-1}\cdot\text{mol}^{-1}$, and $S_m^\circ(\text{acenaphthylene, g}) = 359.1 \text{ J}\cdot\text{K}^{-1}\cdot\text{mol}^{-1}$, at 298.15 K, obtained by the B3LYP/6-31G(d,p) method with frequencies scaled by 0.9620, it is also possible to conclude that $T\Delta_r S_m^\circ(17)$

$= -56.2 \text{ kJ}\cdot\text{mol}^{-1}$ and $T\Delta_r S_m^\circ(18) = -56.3 \text{ kJ}\cdot\text{mol}^{-1}$. Hence, despite the negative entropy contributions, the gas-phase reactions 17 and 18 are considerably exergonic, with $\Delta_r G_m^\circ(17) = -25.2 \text{ kJ}\cdot\text{mol}^{-1}$ and $\Delta_r G_m^\circ(18) = -53.0 \text{ kJ}\cdot\text{mol}^{-1}$ and enthalpically driven. A similar result is obtained for reaction 20. In this case, $\Delta_f H_m^\circ(\text{C}_2\text{H}_4, \text{g}) = 52.5 \pm 0.3 \text{ kJ}\cdot\text{mol}^{-1}$,⁵⁰ $S_m^\circ(\text{C}_2\text{H}_4, \text{g}) = 219.25 \text{ J}\cdot\text{K}^{-1}\cdot\text{mol}^{-1}$,⁵¹ $\Delta_f H_m^\circ(\text{C}_4\text{H}_8, \text{g}) = 27.7 \pm 1.1 \text{ kJ}\cdot\text{mol}^{-1}$,⁵⁰ and $S_m^\circ(\text{C}_4\text{H}_8, \text{g}) = 264.40 \text{ J}\cdot\text{K}^{-1}\cdot\text{mol}^{-1}$ ⁵¹ lead to $\Delta_r H_m^\circ(20) = -77.3 \pm 1.1 \text{ kJ}\cdot\text{mol}^{-1}$, $T\Delta_r S_m^\circ(20) = -51.9 \text{ kJ}\cdot\text{mol}^{-1}$, and $\Delta_r G_m^\circ(20) = -25.4 \text{ kJ}\cdot\text{mol}^{-1}$.



The variation of $\Delta_r G_m^\circ(17)$ and $\Delta_r G_m^\circ(18)$ with temperature (Figure 4) can be predicted by combining the enthalpy of formation of acenaphthylene and the two heptacyclene isomers in the gaseous state shown in Table 2 with the S_m° and $[H_m^\circ(T) - H_m^\circ(0 \text{ K})]$ data obtained for acenaphthylene and *Z*- and *E*-heptacyclene in the range 200–900 K, using the B3LYP/6-31G(d,p) method with vibrational frequencies scaled by 0.9620 (Supporting Information). The obtained results indicate that $\Delta_r G_m^\circ(17)$ and $\Delta_r G_m^\circ(18)$ become positive (endergonic) at 434.0 and 571.2 K, respectively.

Finally, the results presented here suggest that the nonoccurrence of the thermal dimerization of acenaphthylene in the absence of light at 298.15 K has a kinetic origin, in accordance with the Woodward–Hoffmann rules which predict that this thermal dimerization is symmetry forbidden.^{52,53}

MD Simulations. The crystal conformational internal energy at 1 bar, U_{conf}^i , was calculated by MD simulation for acenaphthylene, *Z*-heptacyclene, and *E*-heptacyclene under the three types of force fields mentioned in the Methods section (W&C, OPLS-AA, or OPLS-AA-q) and assuming different regimes of relaxation of the crystal (simulation in the NVT, NpT, or NσT ensembles; see below). The obtained results are shown in Tables 5–7 where U_{conf}^i is the initial configurational energy, (com-

TABLE 5: Energetic and Geometrical Data of Acenaphthylene Crystals Obtained by MD Simulation Methods and Comparison with XRD Data^a

data	XRD ^b	MD								
		OPLS-AA			OPLS-AA-q			W&C		
no. molecules	8									
no. cells	1									
ensemble										
$-U_{\text{conf}}^i$			76.0				72.8		70.4	
Ffield		NVT	NpT	NσT	NVT	NpT	NσT	NVT	NpT	NσT
$-U_{\text{conf}}^\circ$		76.1	73.5	73.8	72.2	68.4	68.7	68.9	69.2	68.9
$\delta U_{\text{conf}}^\circ$		0.4	0.7	0.6	0.4	0.7	0.6	0.6	0.7	0.6
$-U_{\text{vdw}}^\circ$		72.4	70.2	70.4						
$\delta U_{\text{vdw}}^\circ$		0.4	0.6	0.5						
$-U_{\text{coul}}^\circ$		3.7	3.2	3.7						
$\delta U_{\text{coul}}^\circ$		0.1	0.2	0.2						
V	1574		1649	1647	1686	1680		1766	1765	
δV			13	11	13	10		14	12	
a	7.59		7.7	7.7	7.8	7.7		7.9	7.9	
δa			0.2	0.7	0.3	0.8		0.5	0.9	
b	7.46		7.6	7.6	7.7	7.7		7.6	7.6	
δb			0.3	0.5	0.3	0.5		0.4	0.9	
c	27.82		28.3	28.3	28.3	28.2		28.9	28.9	
δc			0.9	1.1	0.9	1.2		1.1	1.3	
β	90.0			90.0		90.1			90.3	
$\delta \beta$				0.9		0.9			1.8	
ρ	1.284		1.226	1.226	1.199	1.203		1.144	1.146	
$\delta \rho$			0.009	0.008	0.009	0.008		0.009	0.008	
$\Delta_{\text{sub}} H_m^\circ$		78.6	75.9	76.3	74.8	70.8	71.2	71.4	71.7	71.4
$\delta \Delta_{\text{sub}} H_m^\circ$		0.4	0.7	0.6	0.4	0.7	0.6	0.6	0.7	0.6

^a Enthalpy and energy data in $\text{kJ}\cdot\text{mol}^{-1}$; unit cell volume, V , in \AA^3 ; cell parameters a , b , and c in \AA and β in degrees; density, ρ , in $\text{g}\cdot\text{cm}^{-3}$.

^b Reference 33.

TABLE 6: Energetic and Geometrical Data of Z-Heptacyclene Crystals Obtained by MD Simulation Methods and Comparison with XRD Data^a

data	XRD ^b	MD								
no. molecules	4	32								
no. cells	1	2 × 2 × 2								
ensemble		OPLS-AA			OPLS-AA-q			W&C		
$-U_{\text{conf}}^i$		137.53			130.16			131.47		
Ffield		NVT	NpT	NoT	NVT	NpT	NoT	NVT	NpT	NoT
$-U_{\text{conf}}^o$		132.1	134.5	134.6	124.8	126.3	126.3	125.5	124.7	124.6
δU_{conf}^o		0.3	0.3	0.6	0.3	0.6	1.6	0.3	0.3	1.3
$-U_{\text{vdw}}^o$		124.7	126.8	126.8						
δU_{vdw}^o		0.3	0.3	0.6						
$-U_{\text{coul}}^o$		7.27	7.63	7.67						
δU_{coul}^o		0.03	0.06	0.09						
V	1588.4		1551	1551	1563	1562		1616	1616	
δV			6	6	6	10		6	6	
a	11.97		11.9	11.8	11.9	11.8		12.0	12.0	
δa			0.3	1.0	0.2	0.5		0.2	1.0	
b	13.93		13.8	13.8	13.9	13.9		14.0	14.2	
δb			0.3	1.3	0.2	0.5		0.4	0.5	
c	10.00		9.9	9.9	9.9	10.0		10.0	10.0	
δc			0.3	0.8	0.1	0.5		0.3	0.5	
β	107.70			107		107				108
$\delta \beta$				3		1				1
ρ	1.26		1.303	1.303	1.294	1.294		1.251	1.251	
$\delta \rho$			0.006	0.006	0.006	0.009		0.006	0.006	
$\Delta_{\text{sub}}H_{\text{m}}^o$		134.6	137.0	137.1	127.3	128.8	128.9	128.0	127.2	127.1
$\delta \Delta_{\text{sub}}H_{\text{m}}^o$		0.3	0.3	0.6	0.3	0.6	1.6	0.3	0.3	1.3

^a Enthalpy and energy data in kJ·mol⁻¹; unit cell volume, V, in Å³; cell parameters a, b, and c in Å and β in degrees; density, ρ , in g·cm⁻³.
^b Reference 5.

TABLE 7: Energetic and Geometrical Data of E-Heptacyclene Crystals Obtained by MD Simulation Methods and Comparison with XRD Data^a

data	XRD ^b	MD								
no. molecules	2	30								
no. cells	1	3 × 5 × 1								
ensemble		OPLS-AA			OPLS-AA-q			W&C		
$-U_{\text{conf}}^i$		150.4			144.6			150.2		
Ffield		NVT	NpT	NoT	NVT	NpT	NoT	NVT	NpT	NoT
$-U_{\text{conf}}^o$		145.2	146.6	151.6	139.8	140.2	148.1	144.3	143.5	150.5
δU_{conf}^o		0.1	0.2	0.3	0.1	0.2	0.2	0.1	0.2	0.2
$-U_{\text{vdw}}^o$		139.8	140.9	147.7						
δU_{vdw}^o		0.1	0.2	0.3						
$-U_{\text{coul}}^o$		5.33	5.650	3.733						
δU_{coul}^o		0.03	0.05	0.06						
V	769.1		757	741	765	746		784	767	
δV			2	3	3	2		2	4	
a	7.83		7.8	7.5	7.8	7.6		7.9	7.7	
δa			0.1	0.7	0.2	0.3		0.2	0.8	
b	4.87		4.8	4.6	4.9	4.5		4.9	4.5	
δb			0.1	0.2	0.1	0.4		0.1	0.3	
c	20.22		20.1	21.5	20.2	21.8		20.4	21.9	
δc			0.3	1.5	0.6	2.0		0.4	1.5	
β	92.79			90.9		90.5				91.6
$\delta \beta$				1.0		1.0				1.6
ρ	1.314		1.333	1.364	1.321	1.355		1.288	1.318	
$\delta \rho$			0.003	0.006	0.006	0.003		0.003	0.006	
$\Delta_{\text{sub}}H_{\text{m}}^o$		147.7	149.1	154.1	142.3	142.7	150.6	146.8	146.0	153.0
$\delta \Delta_{\text{sub}}H_{\text{m}}^o$		0.7	0.3	1.0	0.3	0.7	0.7	0.3	0.7	0.7

^a Enthalpy and energy data in kJ·mol⁻¹; unit cell volume, V, in Å³; cell parameters a, b, and c in Å and β in degrees; density, ρ , in g·cm⁻³. ^b This work.

mon to all ensembles), U_{vdw}^o and U_{coul}^o are the van der Waals and Coulombic contributions to the standard molar configurational internal energy U_{conf}^o , respectively, V is the unit cell volume with a, b, c, and β being the cell parameters, ρ is the density of the crystal, and δ represents the standard deviation of the simulation results obtained during the production cycles. The α and γ director angles of the cells were not included in the tables, since the simulations yielded results that were never significantly different from the initial values of 90°, which

correspond to orthorhombic or monoclinic crystals. In the NVT ensemble runs, the overall geometry of the simulation box was fixed (the length of each side of the box was an integer multiple of the a, b, and c unit cell parameters and the director angles were all the same) and the molecules were allowed to relax inside this constrained geometry. The density was constant during the simulation. In the NpT ensemble, the volume of the simulation box was allowed to change in an isotropic way, that is, the box expanded or contracted while keeping constant the

ratio of the side lengths of the simulation box and the α , β , and γ director angles of the initial configuration. The density varied so that a preselected pressure of 1 bar was attained in all simulations. In the $N\sigma T$ ensemble, the box size and shape were allowed to vary in order to obtain a given pressure (1 bar) and an isotropic stress tensor (σ) in the simulation box. The three ensembles represent successive steps toward an increasingly less constrained relaxation of the crystal. The NpT and $N\sigma T$ runs also yield geometrical data (density and unit cell parameters) for the relaxed crystal, which are compared in Tables 5–7 with data obtained by X-ray diffraction (XRD). For the heptacyclenes, the experimental and calculated volumetric/geometrical data compare very well (the deviations in ρ are smaller than 3%). In the case of acenaphthylene, such comparison is not possible since the selected XRD results correspond to a crystal at low temperature (85 K).³³

The standard molar enthalpies of sublimation of acenaphthylene, *Z*-heptacyclene, and *E*-heptacyclene are related with the conformational internal energy of the crystals by

$$\Delta_{\text{sub}}H_{\text{m}}^{\circ} = -U_{\text{conf}}^{\circ} + RT \quad (21)$$

As seen in Tables 5–7, all models reproduce the experimental $\Delta_{\text{sub}}H_{\text{m}}^{\circ}$ in Table 2 with maximum and average deviations of 8.6 and 3.0 kJ·mol⁻¹ (OPLS-AA), 6.7 and 1.6 kJ·mol⁻¹ (OPLS-AA-q), and 4.0 and 1.2 kJ·mol⁻¹ (W&C), respectively. Note that the inclusion in the OPLS-AA model of point charges that were parametrized to account for nondispersive interactions in the liquid state probably overestimates these interactions in the ordered lattice of a crystal and may explain the poorer accuracy of this force field when compared to the W&C or OPLS-AA-q models.

The effect of relaxation of the crystal is also significant, with U_{conf}° for the fully relaxed $N\sigma T$ structures differing by a few kJ·mol⁻¹ from the corresponding $U_{\text{conf}}^{\text{i}}$ values or the values obtained in runs under NVT or NpT ensembles.

The MD calculations predict a considerably smaller $\Delta_{\text{sub}}H_{\text{m}}^{\circ}$ value for *Z*-heptacyclene than for *E*-heptacyclene, in agreement with the experimental observations. According to the simulations, this difference of ca. 20 kJ·mol⁻¹ can be attributed to the less efficient packing of the molecules in the *Z* crystal due to the “dead volume” that exists between the two planar “acenaphthene” systems formed by the five- and six-membered rings in a *Z* molecule. This dead volume leads to larger than usual distances between atoms of the same molecule belonging to either side of the “acenaphthene” fragments, which means weaker dispersive intramolecular forces. In other words, whereas, in the *E*-heptacyclene crystal, the “acenaphthene” ring systems can always pack forming planar structures on both sides of the rings, in the *Z* crystal, the conformation of the molecule will prevent this from happening. The less efficient packing in the *Z* crystals is evidenced by comparing the corresponding molar density (1.26 g·cm⁻³)⁵ with that of the *E* lattice (1.314 g·cm⁻³, this work), both obtained from XRD experiments. It is also interesting to note that $\Delta_{\text{sub}}H_{\text{m}}^{\circ}$ (acenaphthylene) = 72.97 ± 0.33 kJ·mol⁻¹ (Table 2, 70.8–78.6 kJ·mol⁻¹) is approximately half of $\Delta_{\text{sub}}H_{\text{m}}^{\circ}$ (*E*-heptacyclene) = 149.0 ± 3.1 kJ·mol⁻¹. This suggests that when there are no constraints to the efficient packing of the molecules two dimerized acenaphthylene molecules will interact two times as strongly as a monomeric acenaphthylene system, whereas in the case of *Z*-heptacyclene where a less efficient packing leads to weaker interactions.

Acknowledgment. This work was supported by Fundação para a Ciência e a Tecnologia, Portugal. A grant from Fundação para a Ciência e a Tecnologia (SFRH/BD/12329/2003) is also gratefully acknowledged by C.E.S.B.

Supporting Information Available: Tables with the indexation of the powder diffraction lines for the *E*- and *Z*-heptacyclene samples used in this work. Table with the complete set of bond lengths and bond angles for *E*-heptacyclene. Details of the combustion calorimetry experiments (procedures and results) and tables with the experimental vapor pressures obtained by the Knudsen effusion measurements. Electronic energies, thermochemical corrections, entropies, and $[H_{\text{m}}^{\circ}(T) - H_{\text{m}}^{\circ}(0 \text{ K})]$ values for acenaphthylene, *Z*-heptacyclene, and *E*-heptacyclene obtained by several computational chemistry models. A CIF file with the crystallographic parameters and structural data of *E*-heptacyclene. This material is available free of charge via the Internet at <http://pubs.acs.org>.

References and Notes

- (1) Dzewonski, K.; Rapalski, G. *Chem. Ber.* **1912**, *45*, 2491–2495.
- (2) Dzewonski, K.; Paschalski, C. *Chem. Ber.* **1913**, *46*, 1986–1992.
- (3) Dunitz, J. D.; Weissman, L. *Acta Crystallogr.* **1949**, *2*, 62–63.
- (4) Griffin, G. W.; Veber, D. F. *J. Am. Chem. Soc.* **1960**, *82*, 6417.
- (5) Welberry, T. R. *Acta Crystallogr. B* **1971**, *27*, 360–365.
- (6) Bowen, E. J.; Marsh, J. D. F. *J. Chem. Soc.* **1947**, 109–110.
- (7) Livingston, R.; Wei, K. S. *J. Phys. Chem.* **1967**, *71*, 541–547.
- (8) Hartmann, I.; Hartmann, W.; Schenck, G. O. *Chem. Ber.* **1967**, *100*, 3146–3155.
- (9) Cowan, D. O.; Drisko, R. L. E. *J. Am. Chem. Soc.* **1970**, *92*, 6286–6291.
- (10) Cowan, D. O.; Koziar, J. C. *J. Am. Chem. Soc.* **1975**, *97*, 249–254.
- (11) Dunsbach, R.; Schmidt, R. *J. Photochem. Photobiol., A* **1994**, *83*, 7–13.
- (12) Haga, N.; Takayanagi, H.; Tokumaru, K. *J. Org. Chem.* **1997**, *62*, 3734–3743.
- (13) Haga, N.; Takayanagi, H.; Tokumaru, K. *Photochem. Photobiol. Sci.* **2003**, *2*, 1215–1219.
- (14) Madhavan, D.; Pitchumani, K. *Photochem. Photobiol.* **2003**, *2*, 95–97.
- (15) Laugier, J.; Bochu, B. *Checkcell*; <http://www.ccp14.ac.uk/tutorial/Imgp>.
- (16) Furniss, B. S.; Hannaford, A. J.; Smith, P. W. G.; Tatchell, A. R. *Vogel's Textbook of Practical Organic Chemistry*, 5th ed.; Longman: New York, 1989; p 1240.
- (17) Altomare, A.; Burla, M. C.; Camalli, M.; Cascarano, G.; Giacovazzo, C.; Guagliardi, A.; Moliterni, A. G. G.; Polidori, G.; Spagna, R. *J. Appl. Crystallogr.* **1999**, *32*, 115–119.
- (18) Sheldrick, G. M. *SHELXL-97, A Program for Refining Crystal Structures*; University of Göttingen: Göttingen, Germany, 1997.
- (19) Farrugia, L. J. *J. Appl. Crystallogr.* **1999**, *32*, 837–838.
- (20) Farrugia, L. J. *J. Appl. Crystallogr.* **1997**, *30*, 565, based on ORTEP-III (v.1.0.3.) by C. K. Johnson and M. N. Burnett.
- (21) Bruno, I. J.; Cole, J. C.; Edgington, P. R.; Kessler, M.; Macrae, C. F.; McCabe, P.; Pearson, J.; Taylor, R. *Acta Crystallogr. B* **2002**, *58*, 389–397.
- (22) (a) Calado, J. C. G.; Dias, A. R.; Minas da Piedade, M. E.; Martinho Simões, J. A. *Rev. Port. Quim.* **1980**, *22*, 53–62. (b) Diogo, H. P.; Minas da Piedade, M. E.; Fernandes, A. C.; Martinho Simões, J. A.; Ribeiro da Silva, M. A. V.; Monte, M. J. S. *Thermochim. Acta* **1993**, *228*, 15–22. (c) Diogo, H. P.; Minas da Piedade, M. E.; Gonçalves, J. M.; Monte, M. J. S.; Ribeiro da Silva, M. A. V. *Eur. J. Inorg. Chem.* **2001**, 257–262.
- (23) Kiyobayashi, T.; Minas da Piedade, M. E. *J. Chem. Thermodyn.* **2001**, *33*, 11–21.
- (24) (a) Diogo, H. P.; Minas da Piedade, M. E. *J. Chem. Thermodyn.* **1995**, *27*, 197–206. (b) Santos, R. C.; Diogo, H. P.; Minas da Piedade, M. E. *J. Chem. Thermodyn.* **1999**, *31*, 1417–1427.
- (25) Frisch, M. J.; Trucks, G. W.; Schlegel, H. B.; Scuseria, G. E.; Robb, M. A.; Cheeseman, J. R.; Zakrzewski, V. G.; Montgomery, J. A., Jr.; Stratmann, R. E.; Burant, J. C.; Dapprich, S.; Millam, J. M.; Daniels, A. D.; Kudin, K. N.; Strain, M. C.; Farkas, O.; Tomasi, J.; Barone, V.; Cossi, M.; Cammi, R.; Mennucci, B.; Pomelli, C.; Adamo, C.; Clifford, S.; Ochterski, J.; Petersson, G. A.; Ayala, P. Y.; Cui, Q.; Morokuma, K.; Malick, D. K.; Rabuck, A. D.; Raghavachari, K.; Foresman, J. B.; Cioslowski, J.; Ortiz, J. V.; Baboul, A. G.; Stefanov, B. B.; Liu, G.; Liashenko, A.; Piskorz, P.; Komaromi, I.; Gomperts, R.; Martin, R. L.; Fox, D. J.; Keith, T.; Al-

- Laham, M. A.; Peng, C. Y.; Nanayakkara, A.; Gonzalez, C.; Challacombe, M.; Gill, P. M. W.; Johnson, B.; Chen, W.; Wong, M. W.; Andres, J. L.; Head-Gordon, M.; Replogle, E. S.; Pople, J. A. *Gaussian 98*; Gaussian, Inc.: Pittsburgh, PA.
- (26) Becke, A. D. *J. Chem. Phys.* **1993**, *98*, 5648–5652.
- (27) Perdew, J. P.; Wang, Y. *Phys. Rev. B* **1992**, *45*, 13244–13249.
- (28) Lee, C.; Yang, W.; Parr, R. G. *Phys. Rev. B* **1988**, *37*, 785–789.
- (29) Koch, W.; Holthausen, M. C. *A Chemist's Guide to Density Functional Theory*, 2nd Ed.; Wiley-VCH: Weinheim, Germany, 2002.
- (30) Hariharan, P. C.; Pople, J. A. *Mol. Phys.* **1974**, *27*, 209–214.
- (31) Dunning, T. H. *J. Chem. Phys.* **1989**, *90*, 1007–1023.
- (32) Smith, W.; Forester, T. R. *The DL_POLY Package of Molecular Simulation Routines*, version 2.12; The Council for The Central Laboratory of Research Councils; Daresbury Laboratory: Warrington, U.K., 1999.
- (33) Welberry, T. R.; Rae, A. D. *Proc. R. Soc. London, Ser. A* **1985**, *334*, 19–48.
- (34) Williams, D. E.; Cox, S. R. *Acta Crystallogr. B* **1984**, *40*, 404–417.
- (35) Jorgensen, W. L.; Maxwell, D. S.; Tirado-Rives, J. *J. Am. Chem. Soc.* **1996**, *118*, 11225–11236.
- (36) Ehrlich, H. W. W. *Acta Crystallogr.* **1957**, *10*, 699–705.
- (37) Hazell, A. C.; Hazell, R. G.; Nørskov-Lauritsen, L.; Briant, C. E.; Jones, D. W. *Acta Crystallogr. C* **1986**, *42*, 690–693.
- (38) *IUPAC Commission on Atomic Weights and Isotopic Abundances*; <http://www.chem.qmul.ac.uk/IUPAC/AtW/>.
- (39) Olofsson, G. In *Experimental Chemical Thermodynamics*; Sunner, S., Månsson, M., Eds.; Pergamon Press: London, 1979; Vol. 1, Chapter 6.
- (40) *CODATA Key Values for Thermodynamics*; Cox, J. D., Wagman, D. D., Medvedev, V. A., Eds.; Hemisphere: New York, 1989.
- (41) (a) Edwards, J. W.; Kington, G. L. *Trans. Faraday Soc.* **1962**, *58*, 1323–1333. (b) Andrews, J. T. S.; Westrum, E. F., Jr.; Bjerrum, N. J. *Organomet. Chem.* **1969**, *17*, 293–302.
- (42) Atkins, P. W.; de Paula, J. *Physical Chemistry*, 7th ed; Oxford University Press: Oxford, U.K., 2002; p 822.
- (43) Pascual-Ahuir, J. L.; Silla, E.; Tunon, I. *GEPOL93*; http://server.ccl.net/cca/software/SOURCES/FORTRAN/molecular_surface/gepol93/.
- (44) Cox, J. D.; Pilcher, G. *Thermochemistry of Organic and Organometallic Compounds*; Academic Press: London, 1970.
- (45) Korn, G. A.; Korn, T. M. *Mathematical Handbook for Scientists and Engineers*; McGraw-Hill: New York, 1968.
- (46) Cheda, J. A. R.; Westrum, E. F., Jr. *J. Phys. Chem.* **1994**, *98*, 2482–2488.
- (47) <http://srdata.nist.gov/cccbdb/>; Release 11.
- (48) Diogo, H. P.; Kiyobayashi, T.; Minas da Piedade, M. E.; Burlak, N.; Rogers, D. W.; McMasters, D.; Persy, G.; Wirz, J.; Liebman, J. F. *J. Am. Chem. Soc.* **2002**, *124*, 2065–2072.
- (49) Morawetz, E. *J. Chem. Thermodyn.* **1972**, *4*, 461–467.
- (50) Pedley, J. B. *Thermochemical Data and Structures of Organic Compounds*; TRC Data Series; Thermodynamics Research Center: College Station, TX, 1994; Vol. I.
- (51) *Thermodynamics of Organic Compounds in the Gas State*; Frenkel, M., Marsh, K. N., Wilhoit, R. C., Kabo, G. J., Roganov, G. N., Eds.; Thermodynamics Research Center: College Station, TX, 1994.
- (52) Woodward, R. B.; Hoffmann, R. *The Conservation of Orbital Symmetry*; Verlag Chemie: Weinheim, Germany, 1970.
- (53) Fleming, I. *Frontier Orbitals and Organic Chemical Reactions*; reprinted edition with corrections; John Wiley: Chichester, U.K., 1978.